MODELING LASER IGNITION OF EXPLOSIVES AND PYROTECHNICS: EFFECTS AND CHARACTERIZATION OF RADIATIVE TRANSFER*

R. D. Skocypec, A. R. Mahoney, M. W. Glass,
R. G. Jungst, N. A. Evans, and K. L. Erickson

Sandia National Laboratories
Albuquerque, NM 87185

SAND--90-0577C

DE90 011052

ABSTRACT

The ignition of explosives and pyrotechnics using commercial diode lasers has been demonstrated and is of interest as a potential replacement for hot-wire ignition. Initial laser diode ignitor (LDI) test results using the detonation-to-deflagration transition (DDT) explosive CP (2-(5-cyanotetrazolato)pentaamminecobalt(III) perchlorate, $C_2H_{15}N_{10}Co\text{-}Cl_2O_8$) doped with carbon black and graphite have reinforced the need for a better understanding of the interaction of the radiant energy transfer within the pressed material. The present work is directed toward developing a model to predict the transfer of laser energy in the pressed particulate charges. It is shown here that scattering can have a major effect on the volumetric absorption of laser energy, significantly affecting the thermal response of the granular energetic material.

This paper describes an effort to characterize the radiative properties of compacted granular beds of CP and CP doped with carbon black or graphite that were prepared using normal pressing techniques. Current estimates of the radiative properties are presented and indicate dramatic increases in absorption for CP when even a minute amount of carbon black or graphite is added. Initial data indicate pressed, undoped CP scatters radiative energy significantly. The radiative properties are dependent upon both wavelength and packing density; the less-densely packed samples exhibit more scattering. Doped samples exhibit essentially wavelength-independent characteristics.

These properties are used in a two-flux (scattering) or a simple nonscattering radiative transfer model with conductive heat transfer models to show the effects of scattering on the calculated ignition time (time required for the energetic material to reach "ignition temperature", 300°C). Analyses of the thermal response of the explosive charge during the preignition regime indicate: convective transfer is small, radiative transfer dominates at high power levels (short ignition times) and conductive transfer is critical at low power levels, where two-dimensional effects must be considered to match experimental data. Thus, header design and materials (influencing conductive losses) may be important for LDI operation at low power levels and good radiative property estimates are important to predict high-power operation. In general, the experimental data are matched reasonably well by predictions both in trends and at both the high- and low-power limits investigated.

*This work performed at Sandia National Laboratories supported by the U.S. Department of Energy under Contract DE-AC04-76DP00789.

INTRODUCTION

The ignition of explosives and pyrotechnics using commercial diode lasers has been demonstrated and is of interest as a potential replacement for hot-wire ignition. Initial laser diode ignitor (LDI) test results using the detonation-to-deflagration transition (DDT) explosive CP (2-(5-cyanotetrazolato)pentaamminecobalt(III) perchlorate, $C_2H_{15}N_{10}Co\text{-}Cl_2O_8$) doped with carbon black and graphite have reinforced the need for a better understanding of the interaction of the radiant energy transfer within the pressed material. In addition, decomposition and energetic chemistry, gas product flow, and DDT phenomena are all important mechanisms. Since the energy output of the laser diode is below the ionization or plasma formation threshold, the radiative energy transfer is initially dominated by the absorptance characteristics of the compacted particles. To simplify analyses, many previous investigators have assumed strictly surface absorption of the laser energy [1-3] or volumetric absorption without true scattering effects [4,5], although there is considerable uncertainty in the validity of these assumptions. The present work is directed toward developing an improved model to predict the transfer of laser energy in the pressed particulate charges. It is shown here that scattering can have a major effect on the volumetric absorption of laser energy, significantly affecting the thermal response of the granular energetic material.

This paper describes an effort to characterize the radiative properties of compacted granular beds of CP and CP doped with carbon black or graphite. Both free-standing samples and samples pressed between windows were prepared using normal pressing techniques. A general discussion is presented of the optical characterization of inhomogeneous scattering media (including effects of physical parameters), the extraction of radiative properties from one-dimensional reflection/transmission measurements and the application of these properties to radiative transfer modeling. Inhomogeneous media in this context include any pressed particulate material, comprised of either a single component (e.g., pure CP) or multiple components (e.g., CP and dopant).

These radiative properties are used in models of the thermal response of the granular charge to the laser pulse. One-dimensional, two-dimensional conduction and DDT (multiphase) codes are modified to include radiative transfer within the charge. One large uncertainty is the appropriate chemistry to include. There is also significant uncertainty identifying physical properties of the *as-pressed* charge (such as particle size distribution, particle shape, dopant distribution, etc.) and, as will be shown, there is uncertainty in the radiative properties for the doped material. Consequently, the thermal analysis is intended only to demonstrate observed trends in experimental data and identify important energy-transfer mechanisms that affect the thermal response *prior* to significant chemical activity and thermal runaway (ignition).

RADIATIVE CHARACTERIZATION OF LDI CHARGE MATERIAL

Preliminary characterization of the optical properties of pressed charges of granular CP indicates radiative scattering is significant. Scattering substantially increases

the complexity of characterization, since line-of-sight measurements are no longer adequate (Fresnel reflection analysis is not valid). Generally, absorption is a function of material composition, whereas scattering is influenced by inhomogeneities and discontinuities within the bulk [6]. There are two general approaches to optically characterize these materials: 1) If the optical properties of both the bulk CP and the dopant are known *and* the physical parameters (particle size distribution, particle shape, dopant distribution, etc.) of the *as-pressed* charges are known, then a model can be developed at the discrete particle level;† 2) If these properties are not known, then the materials must be characterized using effective properties that are obtained from optical measurements on macroscopic samples. The effects of discrete particle dopants are, therefore, incorporated in effective properties that are assumed to be homogeneous. The second approach must be used at this time to characterize the LDI charge material. A number of issues regarding the transfer of radiant energy within inhomogeneous media are discussed below.

DIFFUSE VS SPECULAR (REGULAR) REFLECTION

Reflectance is generally a function of the angle of incidence, angle of observation, wavelength, packing density, crystal form, complex refractive index, particle diameter and absorptivity of the component material. The spatial distribution (e.g., surface vs bulk) of these properties can also have a large effect on reflectance. The energy reflected at the interface with inhomogeneous media is typically comprised of both a diffuse and a specular component. These components arise from two different mechanisms: the specular component arises only from surface reflectance, while the diffuse component can arise from both the surface and the interior (especially from the interior in a multiple-scattering medium – discussed below). The ratio of the two components is generally a function of particle size, pressing technique, and the magnitude of the particle absorption coefficient. The specular and diffuse components can be measured (thus providing insight to the primary scattering mechanism – bulk vs surface – in the medium) using a number of techniques. The technique used in this analysis utilizes an integrating sphere to collect both reflectance components. A separate measurement is made in which the specular component exits the integrating sphere through an aperture and only the diffuse component is collected. Subtraction of the two measurements provides the specular component.

Sample material properties and preparation techniques have a large effect on the nature (specular vs diffuse) of the reflectance. Pressing with a flat, hard surface often produces an increase in magnitude of the specular component with pressing pressure due to greater particle orientation. Roughening of the press surface or pressing with a piece of paper between the press and medium has been shown to greatly reduce the specular reflection component.

---

†This type of model may be required in the immediate vicinity of the optical fiber, since a continuum approximation may not be statistically appropriate there. On a purely geometric basis, a 100 μm diameter fiber illuminates ~40 15-μm diameter particles, or ~1000 3-μm diameter particles. Additionally, there are spatial distributions of dopant, laser energy, and density within this domain.

SINGLE VS MULTIPLE SCATTERING

Single scattering occurs when the electromagnetic field interacts with a single particle discontinuity, redirecting energy in all directions. Particles small in size relative to the wavelength (Rayleigh-Gans scattering) scatter energy isotropically and have small scattering cross sections (i.e., they do not scatter large amounts of energy). For densely packed configurations, small-particle scattering is similar to single scattering in that it is isotropic and small in magnitude. However, if aggregates form during any process, the scattering coefficient can dramatically increase (i.e., radiative transfer in small-particle media is highly sensitive to processing techniques). Particle sizes on the order of the wavelength (Mie scattering) and nonspherically shaped particles scatter energy anisotropically. For particles large relative to the wavelength, geometric optics apply and produce predominately forward-directed scattering (e.g., see Refs. [6-10]).

When more than one particle is present, as is generally the case, multiple scattering can occur, in which photons can be redirected more than once within the medium. In the optically thin limit, single scattering predominates and the net scattering effect is obtained by multiplying the single-scattering properties by the number of particles per unit volume. As the optical thickness of the medium increases, this linear relationship with particle number is no longer valid since a greater fraction of energy directed to a given particle comes from other particles, and not directly from the external source. The particles are, however, sufficiently far apart such that the scattering properties of each particle are described by single-scattering properties. This is termed independent scattering and the radiative transfer equations for multiple scattering are valid in this domain.

DEPENDENT VS INDEPENDENT SCATTERING

As the optical thickness of a medium increases further, scattering within the medium becomes more isotropic, independent of the single-scattering anisotropy for the individual particles that constitute the medium. As density increases (particle separation decreases), single-scattering properties no longer adequately represent a given particle due to interference effects from neighboring particles. That is, the far-field solution is no longer appropriate and the standard radiative transfer equations that are based on single-scattering properties are no longer valid. This is termed dependent scattering, and there is no quantitative solution technique at this time, although this is an area of active research. The optically thick, highly scattering, tightly packed LDI charges fall in this category. Presently, the best estimate for the radiative properties can be obtained using a phenomenological approach based on standard multiple-scattering theory using "effective" properties.

SOLVING THE INVERSE PROBLEM FOR RADIATIVE PROPERTIES

One method to determine effective values of the radiative properties is to make reflectance and transmittance measurements on samples of material having different thicknesses. The inverse problem is solved using solutions to the radiative transfer equations to extract a best fit for the properties. Optically thin conditions permit a relatively direct evaluation of single-scattering properties, although the number of

scattering particles must be known. Multiple-scattering conditions require the solution of the radiative transfer equations, in which assumptions are made regarding the directionality (degree of isotropy) of single-particle scattering. If samples are not free-standing and must be pressed onto a window or between two windows to obtain small but finite transmission, corrections for window effects are necessary (this was necessary for the thinner LDI material samples). Radiative property estimates can be used to predict expected reflectance values for the actual ignitor charges, which are optically thick (having no transmission). Absorption coefficients cannot, however, be extracted without finite transmission.

In the present analysis, independent and isotropic scattering is assumed, for which one-dimensional radiative transfer can be characterized using two radiative properties – the single-scattering albedo, $\omega = \sigma_s/\beta$, and the optical depth, $\kappa_L = \beta d$, where β is the extinction coefficient ($= \sigma_s + \sigma_a$), σ_s is the scattering coefficient, σ_a is the absorption coefficient and d is the geometric depth of the medium. The albedo indicates the relative importance of scattering; the larger the albedo, the more significant is the scattering. Generally, each of the properties is a function of wavelength.

EXPERIMENTAL DETERMINATION OF RADIATIVE PROPERTIES

Sample Preparation. A technique similar to that used to produce free-standing pellets of CP explosive was employed to prepare samples for optical characterization. The particulate material was compacted into a metal cup (serving as a form) using a hydraulic-actuated pin. Initially, free-standing samples were prepared by pressing the material into specially machined metal washers to accommodate both optical fixturing and to minimize the amount of material handled for safety considerations. A variety of samples were prepared using this technique by varying the following parameters: packing density (1.5 - 1.7 g/cm^3), particle size (3 and 15 μm), sample thickness (0.381 mm and 0.889 mm), and composition (as-prepared (undoped) and absorbant-doped (graphite or carbon black)). The sample preparation techniques, as well as the measured and calculated optical properties for each sample are listed in Table 1.

In order to achieve better optical measurement sensitivity (i.e, finite transmission), a second set of thinner (0.137 mm - 0.175 mm) samples was prepared using the techniques described above. Since the thinner pellets lacked the mechanical strength to be free-standing, the material was placed between transparent covers and sealed at the edges with adhesive to facilitate handling and optical characterization. Two additional thin samples were made using specially prepared cup assemblies, in which the metal cups were machined to accept a transparent cover material that served as the bottom of the forming cup. The CP material was then placed into these assemblies and compacted.

Instrumentation. The hemispherical reflectance and transmittance properties, covering the wavelength range from 225 nm to 1880 nm, were measured using a Beckman 5270 spectrophotometer equipped with an integrating sphere accessory. The integrating sphere apparatus enables the collection and measurement of the hemispherical reflectance or transmittance; both are comprised of specular and diffuse components.

Additional measurements were performed on a few samples to quantify the diffuse component for both reflectance and transmittance. These measurements were made by opening an aperture on the collection sphere wall to allow the specular component to exit and not be detected. Measured specular-excluded values indicated that the reflectance and transmittance are predominately diffuse. The importance of diffuse reflectance characteristics will be further clarified in the data analysis section below. It should be noted, however, that due to geometrical limitations of the integrating sphere, the sizes of the exit apertures are quite large (reflectance ~135 mrad and transmittance ~150 mrad). Therefore, the specular values measured using this technique are effective values only.

As previously mentioned, thin (0.137 mm - 0.175 mm) CP samples were prepared and encapsulated between transparent cover material. Since the measured optical values are obtained from the complete sample stack (i.e., cover/CP/cover or CP/cover combinations), the influence of the cover material must be accounted for to obtain optical properties for the CP layer itself. The analysis to obtain the necessary corrections is given in Ref. [7].

Data Analysis. Once the hemispherical reflectance[‡], R_H, and transmittance, T_H, values were obtained, either by direct measurement (free-standing samples) or applying corrections (transparent cover samples), the data were analyzed to extract radiative properties using theories of absorption and scattering of tightly packed particles. The Kubelka-Munk (K-M) theory was used since the CP samples constituted packed media having unknown refractive index [8]. The K-M theory is very similar to the Schuster two-flux angular approximation to the radiative transfer equations. Several simplifying assumptions are necessary, including: 1) the scattering distribution of the reflected energy is isotropic (perfectly diffuse – Lambert Cosine Law) so that specular reflectance components are insignificant and can be ignored, 2) the particles that comprise the layer are both homogeneously distributed (σ_a and σ_s are spatially constant), and very much smaller than the layer thickness, and 3) either the layer is subjected to only diffuse irradiation or the reflectance from the layer under perpendicular irradiation is completely diffuse.

In this analysis, R_H and T_H are related to the absorption coefficient, σ_a, and the scattering coefficient, σ_s, by

$$R_H = \frac{(1-\zeta^2)(e^{\gamma d} - e^{-\gamma d})}{(1+\zeta)^2 e^{\gamma d} - (1-\zeta)^2 e^{-\gamma d}} , \tag{1}$$

$$T_H = \frac{4\zeta}{(1+\zeta)^2 e^{\gamma d} - (1-\zeta)^2 e^{-\gamma d}} , \tag{2}$$

where $\gamma = 2\sqrt{\sigma_a(\sigma_a + 2\sigma_s)}$, $\zeta = \sqrt{\sigma_a/(\sigma_a + 2\sigma_s)}$ and d is the sample thickness (mm). The values of σ_a and σ_s that provide the best match to the measured R_H and T_H data are taken as the radiative properties for each sample. For an infinitely thick sample,

[‡]All subsequent variable definitions and equations are functions of wavelength although explicit functional dependency is omitted for clarity.

the transmittance is zero and the reflectance becomes,

$$R(\infty) = \frac{1-\zeta}{1+\zeta}. \tag{3}$$

Finally, in order to quantify the optical influence of adding the absorbant to the undoped CP material, an "effective" surface area factor for the dopant was calculated using $R_3(\infty) = (1-n)R_1(\infty) + nR_2(\infty)$, where $R_1(\infty)$ = diffuse reflectance for an infinite layer thickness of undoped CP, $R_2(\infty)$ = diffuse reflectance for an infinite layer thickness of the dopant material (carbon black or graphite), $R_3(\infty)$ = diffuse reflectance for an infinite layer thickness of the doped CP mixture, and n = the "effective" surface area factor [7]. Solving for n gives,

$$n = (R_3(\infty) - R_1(\infty))/(R_2(\infty) - R_1(\infty)). \tag{4}$$

Values for σ_a, σ_s, β, ω and n are listed in Table 1.

RESULTS

Typical reflectance and transmittance spectra for an undoped CP sample are provided in Fig. 1. This material exhibits reflectance values greater than 0.70 (100% reflectance = 1.00 reflectance unit) over the wavelength range from 600 nm to 1400 nm. Measurement uncertainty is ± 0.02 reflectance/transmittance units due to sample fixture alignment and significantly reduced beam sizes (sample diameters were 6.35 mm and 12.7 mm). Both the hemispherical reflectance, R_H, and transmittance, T_H, values for each sample are listed in Table 1 for three wavelengths of interest (820, 860, and 1060 nm). Most of the undoped CP samples exhibit very small values of σ_a and relatively large values of σ_s, with $\omega > 0.95$. This analysis strongly suggests that the optical properties of the undoped CP material are dominated by scattering, as expected. All values listed in Table 1 have been corrected for window effects (see Ref. [7]). The correction procedure was verified with calibration samples.

Undoped CP. The accuracy and reliability of the calculated values in Table 1 depends on having finite transmission (values above $\sim$0.06). Since the T_H values for the 0.889 mm-thick samples are negligible, results from these measurements are less reliable and these data are not listed in Table 1. In general, the data show a dependency on λ: as wavelength increases (from 820 to 1060 nm), the albedo, ω, increases and the absorption coefficient, σ_a, decreases. The lower absorption coefficient indicates less volumetric absorption (greater depth of penetration of incident energy) and the increase in albedo indicates that relatively more scattering occurs (indicated by the increase in measured reflectance). Note that there can be a strong effect of the albedo on radiative predictions (e.g., comparing the 860 nm data for the first undoped CP, 15 μm sample with the graphite-doped sample, a 16% decrease in ω produces a 37% decrease in reflectance). The 15 μm data, when compared to the 3 μm data, show a slight increase in both albedo and extinction coefficient. In this case, although the reflectance values are similar, the energy is absorbed somewhat closer to the irradiated surface for the 3 μm material.

The comparison between particle sizes is qualitative at best since reproducibility of the 3 μm particle samples is not good and not enough samples were available to accurately quantify the characteristics. Also, some samples had surface discoloration, indicating possible particle agglomeration. Greater preparation sensitivity for small particle material was discussed earlier (see p. 4) and appears to be valid for the LDI material. Increased packing density produced less reproducibility, possibly due to greater alteration of the original material properties. The larger particle material was more reproducible and no surface discoloration was observed.

Average properties for the 15 μm undoped CP material at the wavelengths of interest are listed in Table 1. The "best" values for undoped CP at 820 nm are: ω =0.969 and σ_a =0.48 mm^{-1}.

Doped CP. The data for carbon black-doped CP samples are listed in Table 1, with a single graphite-doped sample for comparison. All T_H values are lower than desired for accurate property evaluation, even for the 0.17 mm-thick samples on windows, but qualitative trends can be extracted. The properties for these samples are estimates only. Much thinner samples, prepared using both varied dopant concentration and packing density, are necessary to obtain more quantitative data. The difficulty in obtaining adequate sample configurations to permit extraction of properties from highly absorbing materials is a well-documented problem [7].

In general, the doped samples have a large decrease in albedo (and reflectance) and a significant increase in absorption coefficient. Relative to undoped CP, doped samples exhibit less wavelength-dependency over the range investigated and the effect of particle diameter or packing density was not evaluated. Compared to the undoped CP, the graphite-doped sample has a marginal decrease in ω and a much larger σ_a, although the accuracy of the absorption coefficient is in question due to the extremely low T_H values for this sample. The carbon-black doped material exhibits a significant decrease in albedo and the absorption coefficient increases by a factor of $\sim$20, indicating that absorption is dramatically enhanced toward the illuminated side of the sample. The 0.381 mm-thick sample has lower σ_a values that we believe are due to optically thick conditions. Presently, the best estimates for the optical properties for 0.8% carbon-black doped CP at 820 nm are: ω =0.281 and σ_a =9.2 mm^{-1}.

The parameter that indicates the effectiveness of the dopant is the effective surface area factor, n, listed in Table 1. The $R_2(\infty)$ values needed in Eq. (4) for graphite and carbon black were measured to be 0.13 and 0.03, respectively. The area factors for the 0.8% graphite- or carbon-black-doped CP are =0.38 and =0.85, respectively. These factors are in general agreement with microscopic observations on similarly prepared samples. *This* factor (not the weight percent loading) is the parameter that indicates the effect of adding inhomogeneous dopants, and demonstrates the effectiveness of carbon-black as a dopant. This factor incorporates the difference in distribution and size of the dopants.

These radiative properties are used in the following thermal analyses to demonstrate how they can significantly affect the thermal response of the explosive when irradiated by a diode laser pulse. Due to large uncertainties in the appropriate chemistry, the physical properties of the *as-pressed* charge, and radiative properties for the doped material, comparisons to experimental data are not intended to be for validation purposes. The thermal analyses are intended only to demonstrate observed trends in experimental data and identify important energy-transfer mechanisms that affect the thermal response *prior* to significant chemical activity and thermal runaway (ignition).

The thermal response of the charge material during this pre-ignition regime is expected to be dominated by the volumetric absorption of the laser energy and conductive energy transfer both within the charge and to the charge holder. The effect of assuming surface absorption of the laser power was first evaluated. Results indicated the charge would ignite within times that were orders of magnitude shorter than those observed experimentally. Temperatures are relatively low, so infrared radiative transfer should be small. Gas release occurs primarily during ignition, suggesting that convective transfer during pre-ignition should be small. A rigorous multiphase DDT model [11] was modified to include radiative transfer (with scattering) in the charge. Results indicated convective heating during the pre-ignition regime was negligible. Consequently, a transient conduction model of the solid phase with volumetric radiative absorption is applied. The effect of scattering is demonstrated by including either a purely absorbing radiative model or a radiative model that includes scattering.

The one-dimensional approximation is given by,

$$\rho C_p \frac{\partial T}{\partial t} = k(1-\phi)\frac{\partial^2 T}{\partial z^2} + q_{rad}(z) \ , \tag{5}$$

where ϕ is the porosity of the charge (void volume per unit volume of the charge) and $q_{rad}(z)$ is the volumetric absorption of the incident laser power. For a purely absorbing charge, $q_{rad}(z)$ is defined as,

$$q_{rad}(z) = \frac{\tau\beta P}{A}\exp(-\beta z) \ , \tag{6}$$

where τ is the surface transmittance (1 - surface reflectance) (0.16 for undoped CP and 0.85 for CP doped with carbon black), β is the extinction coefficient (from Table 1), P is the laser power incident to the charge, and A is the area of the laser beam. For a charge that scatters and absorbs laser power, $q_{rad}(z)$ is determined using a two-flux technique. The two-flux technique approximates radiative transfer by grouping the radiant energy into either a positive-directed hemispherical flux ($q^+(z)$) or a negative-directed hemispherical flux ($q^-(z)$) [12]. The volumetric absorption is determined from,

$$q_{rad}(z) = \beta m(1-\omega)(q^+(z) + q^-(z)) \ , \tag{7}$$

where $m = \sqrt{3}$ and ω is the single scattering albedo (from Table 1).

For an isotropically scattering medium,

$$\frac{dq^+(z)}{dz} = -\beta m(1 - \frac{\omega}{2})q^+(z) + \beta\frac{m\omega}{2}q^-(z), \tag{8}$$

$$\frac{dq^-(z)}{dz} = -\beta\frac{m\omega}{2}q^+(z) + \beta m(1 - \frac{\omega}{2})q^-(z). \tag{9}$$

At the illuminated side of the charge, the laser flux is specified by considering the interaction with the optical fiber. The incident laser flux is assumed to be uniform. The boundary condition that includes interaction with the fiber is,

$$q^+(0) = P + \rho_f q^-(0), \tag{10}$$

where ρ_f is the reflectance of the optical fiber interface (0.05). At the end of the charge, an adiabatic radiative boundary condition is specified,

$$q^+(L) = q^-(L). \tag{11}$$

RESULTS

As described in Ref. [13], the LDI test device consisted of a pressed charge column 0.25 cm in length, 0.22 cm diameter, with the energy from a commercial 2 watt (GaAl)As diode laser (775 - 850 nm wavelength) delivered by a 100 μm diameter optical fiber directly to the charge. The delivered power is variable. Two charge materials were considered, 15 μm undoped CP and 15μm CP doped with 0.8% carbon black, each having a density of 1.7 gm/cm^3.

Figures 2 and 3 show the volumetric absorption of the laser power, q_{rad}, as a function of distance into the charge. Figure 2, for the undoped 15 μm CP, shows how scattering is significant and distributes the radiative power through a greater portion of the charge (two-flux results with average properties from Table 1 at 820 nm) relative to the pure absorption model (with average extinction coefficient from Table 1 at 820 nm). In contrast, in Fig. 3 the two models are applied to the 15 μm CP doped with 0.8% carbon black and similar penetration into the charge is predicted, due to the significant decrease in scattering from the carbon black dopant (average properties taken from Table 1 at 820 nm). Noting the change in scale of the abscissa, the penetration of laser power is greatly reduced for the doped charge material.

To determine the effect of differences in radiative absorption on the thermal response of the charge and to compare predicted results with experimental data, minimum ignition energy vs laser power curves were generated using the two-flux radiation model in Eq. 5. A typical experimentally determined curve is shown in Fig. 4 for a 1% carbon black loading. Two asymptotic limits are observed. Since the delivered energy is the time integration of the delivered power, short function times occur at high power and longer function times at low-power conditions. For LDI experimental data (having function times 0.1 - 100 ms), predicted ignition times can be compared to experimental function times (which include ignition and DDT) since DDT occurs within microseconds. That is, function times and ignition times are comparable within microseconds. Predicted and experimentally determined minimum energy vs laser power curves can be compared with similar accuracies.

A number of boundary conditions were examined at the fiber/charge interface: (1) adiabatic, (2) the optical fiber having thermal properties of pyrex glass in solid contact with the charge, and (3) a thin film of mylar placed between the fiber and the explosive charge (reducing the conductance losses). The mylar has a high transmittance and is assumed to have a negligible effect on the divergence of the incident laser power. Figures 5 and 6 show the predicted energy-power curves for the two charge materials. "Ignition" is assumed to occur when the charge material reaches 300°C, based upon differential scanning calorimetry data [14]. The undoped CP shows a large dependency on the conductive boundary condition at all power levels investigated, while the doped charge exhibits a large dependency primarily at lower power levels (long ignition times). As expected, the lowest minimum energies are required for adiabatic conditions, followed by reduced conductive losses with the mylar and the highest energies are required for the fiber directly in contact with the charge. A significant decrease in minimum ignition energies are observed for the doped charge relative to the undoped CP (as is observed experimentally).

When comparing the predicted curves (for 0.8% carbon black) to the experimentally determined curves (for 1.0% carbon black), the general shape of the curves are similar, although the predicted curves indicate ignition occurs even for very small power levels whereas this is not experimentally observed. At the low power levels (long ignition times), two-dimensional heat transfer effects may become important. To account for two-dimensional conductive transfer, the first term on the right side of Eq. 5 was extended to two dimensions, although the two-flux radiative absorption term is not rigorously extended. q_{rad} is given as,

$$q_{rad}(r,z) = q_{rad}(z) \quad \text{for} \quad r < R_f \tag{12}$$

$$= 0 \qquad \text{for} \quad r > R_f, \tag{13}$$

where R_f is the radius of the fiber optic. This model is applied to the doped CP charge and the power/energy curves (using properties for 0.8% carbon black) are shown in Fig. 7. The power/energy curves more closely match the experimental data and the two-dimensional effects dramatically increase the minimum ignition energies at low power levels. Considering the uncertainty in properties and the relatively simple model, the experimental data are matched reasonably well both in trends and at both asymptotes.

CONCLUSIONS

The data and analysis presented in this paper, based on an approximate solution to the radiative transfer equations, indicate that pressed undoped CP scatters radiative energy significantly. We are relatively confident in the radiative properties and trends obtained for pressed 15 μm undoped CP. The "best" estimates for the radiative properties of this material are (at 820 nm): single-scattering albedo =0.969, absorption coefficient = 0.48 mm^{-1}. The radiative properties are dependent upon both wavelength and packing density; the less-densely packed samples exhibit more scattering. Good sample reproducibility is observed for this material. In contrast, sample reproducibility must improve for the 3 μm CP if accurate properties are to

be obtained. This material is also more sensitive to packing density and wavelength than the 15 μm CP. These three trends are expected for pressings of smaller-diameter particle material.

The addition of dopants (especially carbon black) dramatically decreases the albedo and increases the absorption coefficient, indicating scattering decreases and absorption is significantly enhanced within the material toward the illuminated side. Doped samples exhibit essentially wavelength-independent characteristics. Due to greater absorptance, samples thinner than measured to date (0.17 mm) are required to adequately characterize the radiative properties of doped CP. The "best" estimates for 15 μm CP doped with 0.8% carbon black are (at 820 nm): single-scattering albedo =0.281, absorption coefficient = 9.2 mm^{-1}.

Since the absorptivity of carbon black is almost unity and the undoped CP is such a poor absorber, the addition of even a minute amount of absorber dramatically affects both the scattering and absorption characteristics within the media. The effect of adding dopant is quantified by the "effective" dopant surface area factor, n. For dopant levels of 0.8% graphite, n =0.38 and for 0.8% carbon black, n=0.85, indicating that ~85% of a given cross section of a carbon-black-doped charge is covered with carbon black. This is partly due to the very small (submicron) size of the dopant. The large effective surface area factor suggests that increasing the dopant level above 0.8% for carbon black may not yield significant increases in laser absorptance, and may eventually decrease response by depleting the energetics of the charge. This has been verified experimentally [13].

Since the material configuration (i.e., packing density, surface topology, etc.) of the samples prepared for optical characterization may not be the same as that of the actual charges, reflectance measurements on the actual charge assemblies is necessary to verify the observed trends and radiative properties. Additional measurements and refined analyses are also suggested if estimates of the spatial distributions of physical parameters are to be made at as detailed a level as possible.

Analyses of the thermal response of the explosive charge during the preignition regime indicate: convective transfer is small, radiative transfer dominates at high power levels (short ignition times) and conductive transfer is critical at low power levels, where two-dimensional effects must be considered to match experimental data. Thus, header design and materials (influencing conductive losses) may be important for LDI operation at low power levels and good radiative property estimates are important to predict high-power operation. In general, the experimental data compare reasonably well both in trends and at both asymptotes to model predictions.

ACKNOWLEDGEMENTS

The authors gratefully acknowledge the assistance of C. E. Haynes at Sandia National Labs for preparation of samples for radiative property measurement.

DISCLAIMER

REFERENCES

1) Boddington, T., Feng, C. and Gray, F., *Archivum Combustionis*, 5: 61 (1985).

2) Chow, C. T. S. and Mohler, J. H., *G. T. P. S.*, 55 (1987).

3) Demming, J. L., Weber, J. H. and Tao, L. C., *Combustion & Flame*, 14: 375 (1970).

4) Harrach, R. J., *J. Appl. Phys.*, 47 (6): 2473 (1976).

5) Merzhanov, A. G. and Averson, A. E., *Combustion & Flame*, 16: 89 (1971).

6) Bohren, C. F. and Huffman, D. R., Absorption and Scattering of Light by Small Particles, John Wiley and Sons (1983).

7) Kortüm, G., Reflectance Spectroscopy, Springer-Verlag (1969).

8) Egan, W. G. and Hilgeman, T. W., Optical Properties of Inhomogeneous Materials, Academic Press (1979).

9) van de Hulst, H. C., Light Scattering by Small Particles, Dover Publ. (1981).

10) Kerker, M., The Scattering of Light and Other Electromagnetic Radiation, Academic Press (1969).

11) Baer, M. R., Gross, R. J. and Nunziato, J. W., *Combustion & Flame*, 65: 15-30 (1986).

12) Özisik, M. N., Radiative Transfer and Interactions with Conduction and Convection, John Wiley & Sons (1973).

13) Jungst, R. G., Salas, F. J., Watkins, R. D. and Kovacic, L., *Proc. 15th International Pyrotechnics Seminar* (July 9-13, 1990).

14) Searcy, J. Q. and Shanahan, K. L., *Sandia National Labs Report SAND78-0466* (Aug. 1978).

Table 1. Radiative Properties of Undoped and Doped CP Charge Material

ρ (g/cm^3)	S*	d (mm)	λ (nm)	$R_H^\dagger$	$T_H^\dagger$	σ_a (mm^{-1})	σ_s (mm^{-1})	β (mm^{-1})	ω	n
Undoped CP, 3 μm										
1.5	FS	0.381	820	0.76	0.03	0.47	11.83	12.3	0.962	
			860	0.79	0.05	0.35	11.25	11.6	0.970	
			1060	0.80	0.10	0.17	8.43	8.6	0.980	
1.7	FS‡	0.381	820	0.49	0.20	0.55	2.45	3.0	0.817	
			860	0.52	0.24	0.39	2.41	2.8	0.861	
			1060	0.51	0.29	0.36	2.04	2.4	0.849	
Undoped CP, 15 μm										
1.5	FS	0.381	820	0.79	0.02	0.44	15.26	15.7	0.972	
			860	0.82	0.03	0.32	15.48	15.8	0.980	
			1060	0.86	0.05	0.17	14.93	15.1	0.989	
1.6	DC	0.137	820	0.74	0.15	0.45	15.15	15.6	0.971	
			860	0.75	0.18	0.31	13.69	14.0	0.978	
			1060	0.74	0.23	0.12	11.39	11.5	0.990	
1.6	DC	0.155	820	0.74	0.16	0.36	12.64	13.0	0.972	
			860	0.75	0.19	0.21	11.59	11.8	0.982	
			1060	0.74	0.26	0.07	9.23	9.3	0.992	
1.7	FS	0.381	820	0.75	0.01	0.67	16.43	17.1	0.961	
			860	0.80	0.04	0.35	13.46	13.8	0.975	
			1060	0.82	0.06	0.20	11.10	11.3	0.982	
average values			820			0.48	14.92	15.4	0.969	
			860			0.29	13.61	13.9	0.979	
			1060			0.14	11.66	11.8	0.988	
CP doped with 0.8% graphite, 15 μm										
1.5	FS	0.381	820	0.52	0.0	2.14	9.76	11.9	0.820	0.38
			860	0.52	0.0	2.14	9.76	11.9	0.820	0.41
			1060	0.50	0.0	2.24	8.86	11.1	0.798	0.48
CP doped with 0.8% carbon black, 15 μm										
1.5	FS	0.381	820	0.17	0.01	4.19	2.01	6.2	0.325	0.82
			860	0.17	0.01	4.31	2.09	6.4	0.327	0.82
			1060	0.16	0.01	4.71	2.19	6.9	0.318	0.84
1.6	DC	0.170	820	0.18	0.01	8.62	4.58	13.2	0.347	0.80
			860	0.17	0.01	8.93	5.07	14.0	0.362	0.82
			1060	0.16	0.01	8.99	4.41	13.4	0.329	0.83
1.6	SC	0.175	820	0.11	0.01	9.73	2.67	12.4	0.215	0.89
			860	0.11	0.01	9.53	2.77	12.3	0.225	0.89
			1060	0.12	0.01	10.07	3.03	13.1	0.231	0.90
average values			820			9.20	3.60	12.8	0.281	0.85
			860			9.32	3.88	13.2	0.294	0.86
			1060			9.58	3.72	13.3	0.280	0.87

* S = sample condition, FS = free-standing, DC = sample between 2 transparent covers, SC = sample on single transparent cover (back); † measured values; ‡ visible surface discoloration

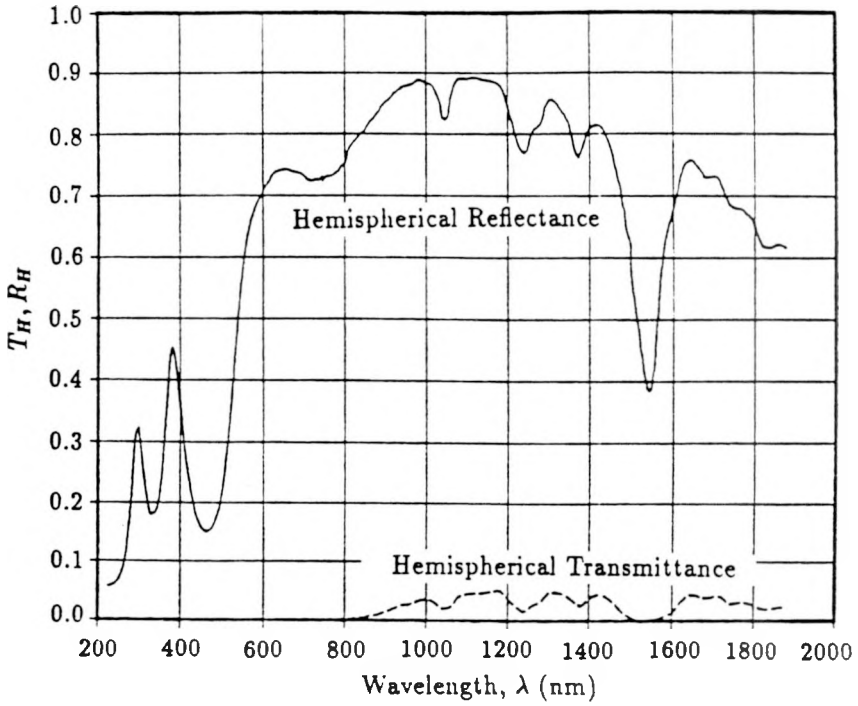

Figure 1. Spectral hemispherical reflectance and transmittance of undoped CP; sample thickness =0.889 mm.

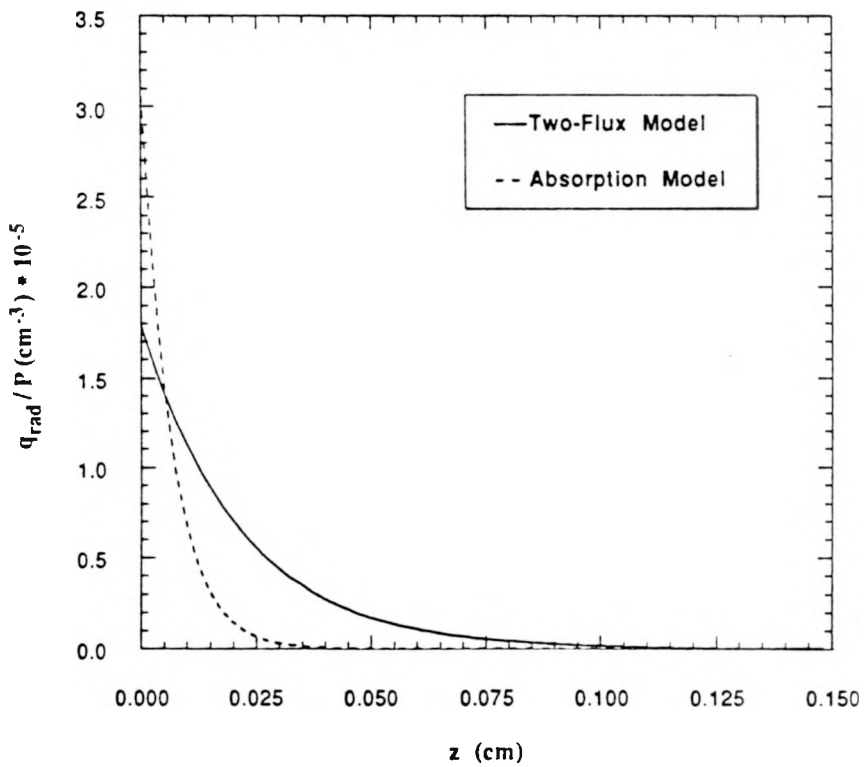

Figure 2. Distribution of laser power volumetric absorption with distance into charge of 15 μm undoped CP when scattering is included (two-flux model) or when scattering is ignored (absorption model).

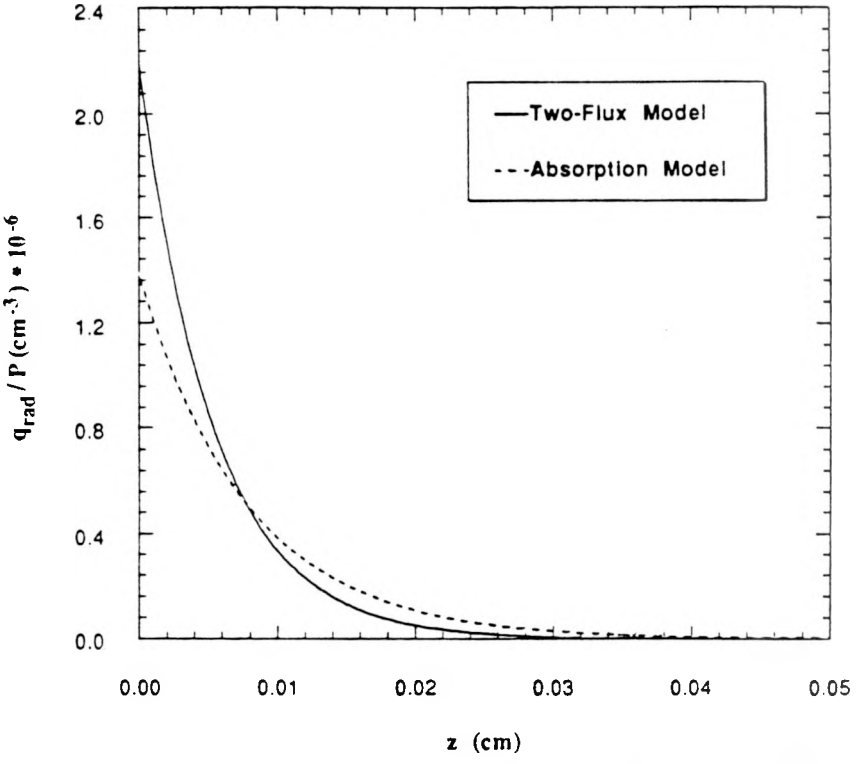

Figure 3. Distribution of laser power volumetric absorption with distance into charge of 15 μm CP doped with 0.8% carbon black when scattering is included (two-flux model) or when scattering is ignored (absorption model).

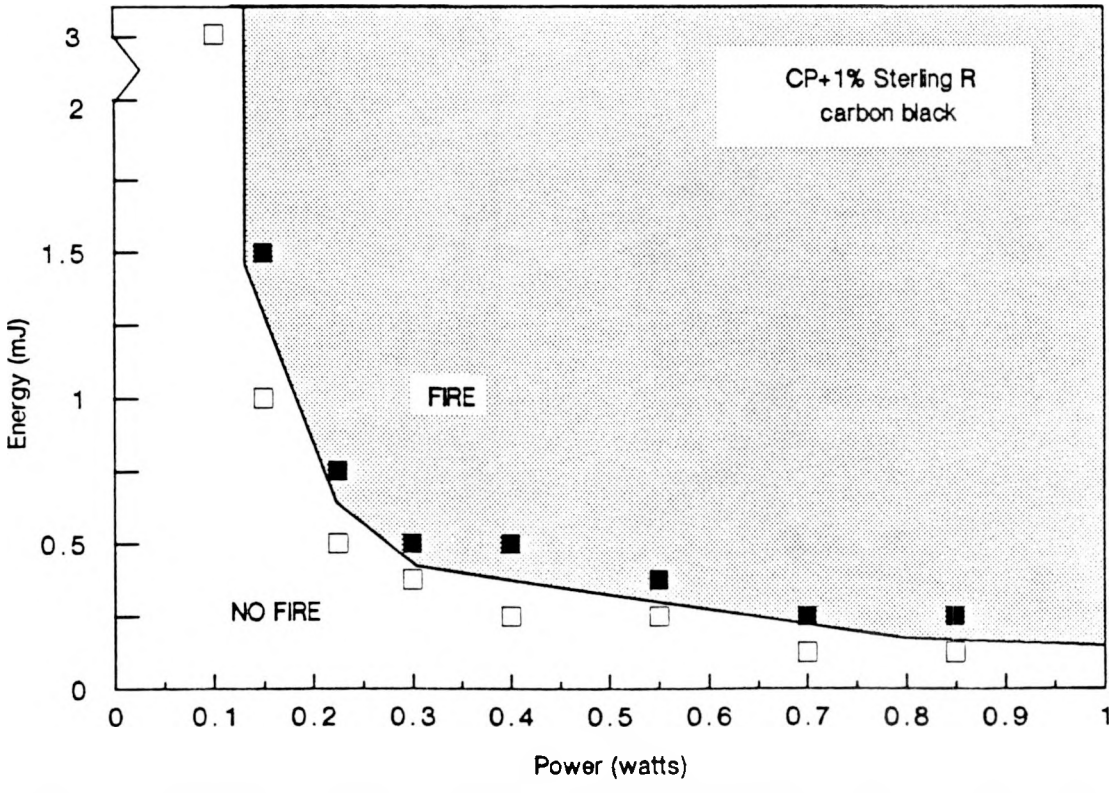

Figure 4. Minimum energy vs incident laser power for 15 μm CP doped with 1% carbon black – experimental data.

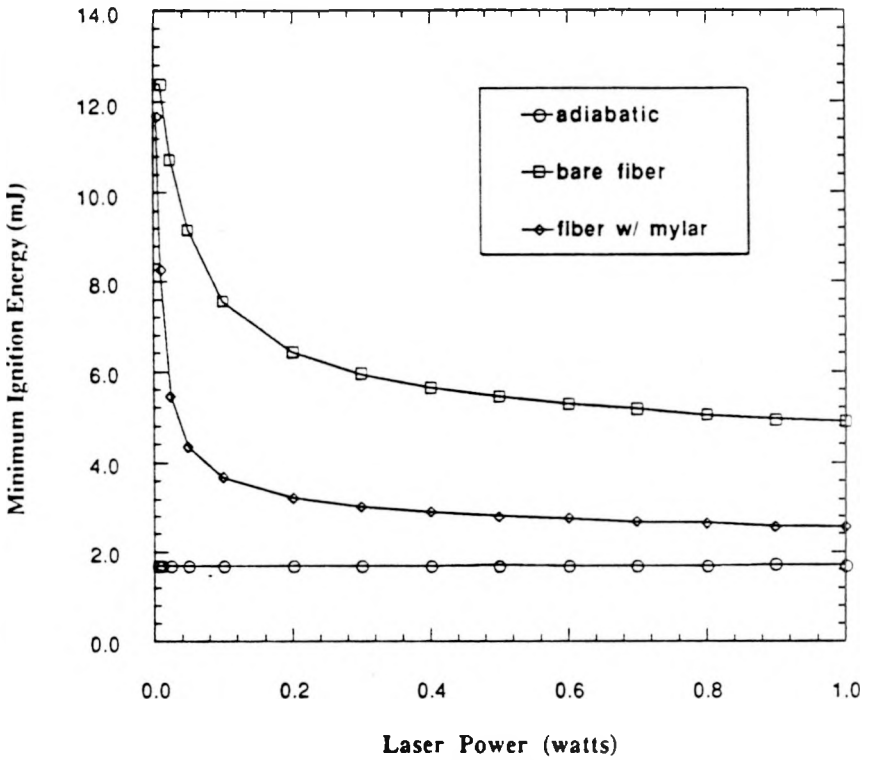

Figure 5. Minimum ignition energy vs incident laser power for 15 μm undoped CP – one-dimensional model predictions.

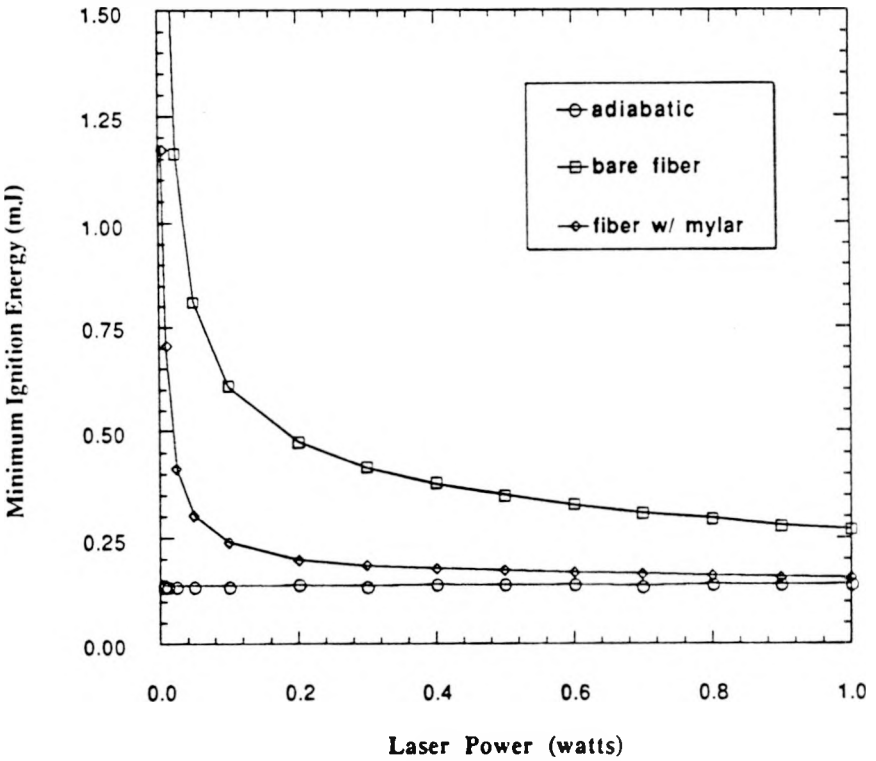

Figure 6. Minimum ignition energy vs incident laser power for 15 μm CP doped with 0.8% carbon black – one-dimensional model predictions.

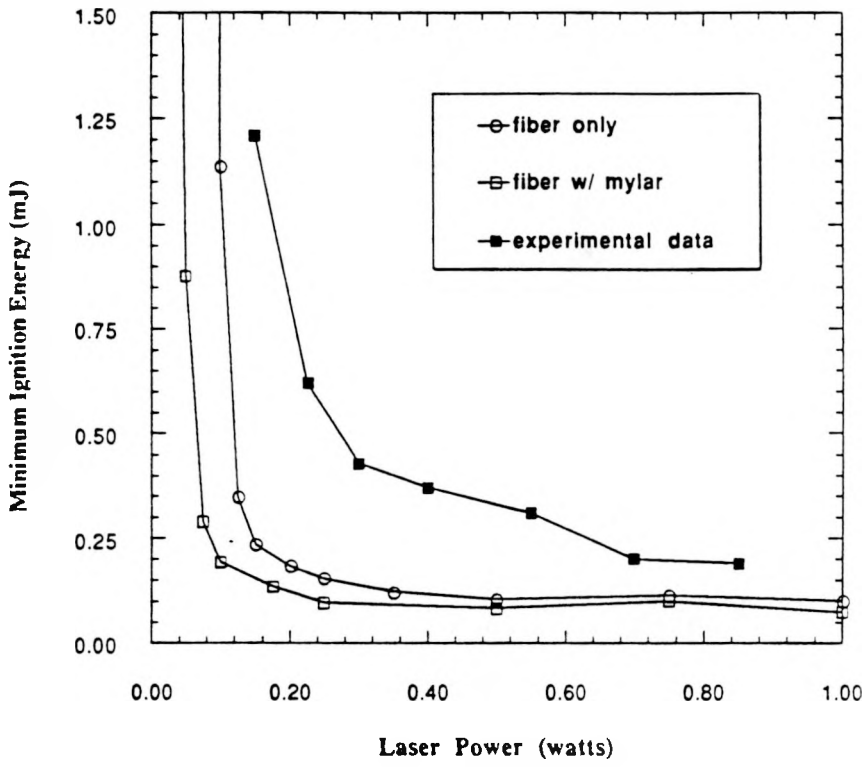

Figure 7. Minimum ignition energy vs incident laser power for 15 μm CP doped with 0.8% carbon black – two-dimensional model predictions.